

# Observation of the vortex lattice spinodal in NbSe<sub>2</sub>

<sup>1,3</sup>Z. L. Xiao, <sup>1</sup>O. Dogru, <sup>1</sup>E. Y. Andrei, <sup>2,4</sup>P. Shuk and <sup>2</sup>M. Greenblatt

<sup>1</sup>Department of Physics and Astronomy, Rutgers University, Piscataway, NJ 08855

<sup>2</sup>Department of Chemistry Rutgers University, Piscataway, NJ 08855

<sup>3</sup>National Laboratory, Chicago, Illinois 60439

<sup>4</sup>Emerson Process Management Rosemount Analytical Inc.

Metastable superheated and supercooled vortex lattices in NbSe<sub>2</sub> crystals were probed with fast transport measurements over a wide range of field and temperature. The limit of metastability of the superheated vortex lattice defines a line in the phase diagram that lies below the superconducting transition and is clearly separated from it. This line is identified as the spinodal for the superheated vortex lattice and is in good agreement with recent theoretical predictions. By contrast no limit of metastability is observed for the supercooled lattice.

7425Dw, 7425Fy, 7425Bt

Systems of many interacting particles often exhibit metastability and irreversible behaviour that betray the presence of local minima in the free energy landscape. In the vicinity of a first-order transition these local minima can trap the system in a metastable superheated or supercooled, “wrong” phase<sup>1</sup>. The metastable region extends up to the spinodal, a line in the phase diagram that demarcates the limit of stability with respect to fluctuations toward the thermodynamically stable state. In recent years, it was found that

vortices in superconductors<sup>2</sup> provide a striking example of such a system with metastability manifesting itself in supercooling<sup>3, 4</sup> and superheating<sup>5</sup> as well as in more surprising ways such as frequency memory<sup>6</sup> and nonlinear dynamics<sup>7-9</sup>. These phenomena appear in conjunction with a sudden increase in the critical current as a function of field or temperature, the so-called peak effect<sup>10, 11</sup>, which is attributed to an order-disorder transition in the vortex lattice<sup>11-15</sup>. Although the region of metastability associated with this transition is observed in many experiments there is to date no evidence of a spinodal line. In this letter we report results of transport measurements on a superheated vortex lattice that identify for the first time a spinodal line above which the system becomes reversible.

The thermodynamically stable state of a type II superconductor in a magnetic field at low temperatures is a lattice of vortices with quasi long-range-order (Bragg glass<sup>17</sup>). As the temperature is raised the vortex lattice undergoes a first-order transition<sup>18, 19</sup> to a stable disordered state. Transport measurements provide a fast and accurate way to determine the degree of order in the vortex lattice, even for very small samples, from the critical current,  $I_c$ , where vortices first start moving and dissipation sets in<sup>11</sup>.  $I_c$  decreases with increasing degree of order as characterized by the size of coherent domains<sup>11</sup>. Thus at low temperatures where the lattice is ordered,  $I_c$  is lower than for the disordered lattice at high temperatures resulting in the peak effect<sup>10, 11</sup>. Standard transport measurements often probe a vortex lattice that has undergone some type of current-induced-organization rather than the initial state<sup>20-22</sup>. This is because during such measurements vortices have enough time to move and reorder in response to the driving current. Current-induced-

organization can result in a more disordered lattice due to “edge contamination”<sup>23, 24</sup> by new vortices entering through a surface barrier at the sample edge, or in a more ordered lattice due to “motional ordering” when vortices are driven at high velocities<sup>25</sup>.

To avoid current-induced-organization we developed a technique that probes the vortex response on time scales shorter than reorganization times and can capture the response of the initial (static) vortex state much like a snapshot. The technique, employs a four-probe measurement to monitor the vortex response to an applied current ramp<sup>20</sup>. The ramps used in most measurements discussed here were Fast-Current-Ramps (FCR) with a sweeping-rate of 200A/s. When a standard Slow-Current-Ramp (SCR) was used, the sweep-rate was 1mA/s. The sweep-rate controls the degree of current-induced-organization. In the case of SCR the measurement time to obtain a voltage signal within our resolution of  $\Delta V \sim 1 \mu V$  is  $\tau = \Delta V / (R_{ff} dI/dt) \sim 0.4s$  for a free flux flow resistance of  $R_{ff} = 2.5 m\Omega$ . This is much longer than the time it takes a vortex to traverse the entire sample (typically  $\sim 50ms$  at 0.25T and 5 $\mu V$ ) so current-induced-organization is inevitable. By contrast if the same vortex is probed by FCR, where  $\tau \sim 2 \mu s$ , it moves less than half a lattice spacing. The FCR were sufficiently fast to capture the intrinsic response of the vortex lattice below the peak effect but they were still too slow close to the peak. We found that it is possible to capture the intrinsic response in the peak region by using the modified method as described below.

The experiments were carried out on three single crystals of 2H-NbSe<sub>2</sub> with critical temperatures  $T_c = 5.61$  K, 7.01 K and 6.0 K for sample A, B and C respectively and  $I_c$  was defined as the current for which the response reaches 5  $\mu V$ . In Fig.1, we show the temperature dependence of  $I_c$  for vortex lattices prepared by several methods: 1.

Supercooled lattice prepared by Field-Cooling (FC), whereby the field is applied prior to cooling through the superconducting transition temperature,  $T_c$ . In this processes, as superconductivity takes over, the field in the sample coalesces to form vortices, which remain in a supercooled disordered state at lower temperatures as indicated by the high values of  $I_c$ . Below the peak, the FC state is metastable. Any disturbance causes it to decay quickly into the ordered state as indicated by the arrow.

2. The Zero-Field-Cooled (ZFC) lattice is prepared by applying the field after cooling to the desired temperature. In this case, vortices penetrate from the periphery moving into the sample at high speeds and forming a motionally ordered state. This is reflected in the values of  $I_c$  which are significantly lower than in the FC case. We note that the width of the peak depends on measurement speed<sup>21</sup>. For the slow SCR the peak is broadened by edge contamination while for the FCR where current-induced-organization is negligible the peak is narrower.

3. The superheated lattice was obtained by a ZFC-Warm (ZFCW) process, which entails preparing the ZFC lattice at a temperature  $T_0$  well below the peak effect, and then heating it to the target temperature  $T_1$  where it is allowed to thermalize for 2-3 minutes. The peak for the ZFCW lattice shifts to higher temperatures compared to the ZFC as expected for a superheated lattice. However, the corresponding  $VI$  curves close to the peak temperature were N-shaped, as shown in Fig. 2, which is a signature of current induced organization<sup>9, 21</sup>. . Since this indicates that the FCR is still too slow in the peak regime we followed a different procedure: the ZFCW lattice was not probed at  $T_1$  but, after waiting at  $T_1$  for a few minutes it was cooled back to  $T_0$  and measured with FCR. The critical currents obtained by this procedure, henceforth referred to as “cold-measured-critical-currents” and labeled  $I_{cc}(T_1)$ , are shown in Fig.3 by solid circles. They were used to calculate (as

described below) the values of  $I_c(T)$  for the ZFCW state, also shown in Fig. 1. The ZFCW peak occurs at a higher temperature and is narrower than in the case of the ZFC lattice. The ZFCW lattice is metastable decaying into the disordered state under external perturbations as indicated by the arrow.

In Fig. 3 we note that at low temperatures  $I_{cc}(T_I)$  for the ZFCW data remains constant and equal to the critical current of the ordered state for up to an onset temperature where it starts increasing and ultimately saturates at the value of the disordered state at  $T_s \sim 5.18\text{K}$ . For comparison, we also plot data obtained with other procedures: plain-ZFC, prepared at  $T_I$  but measured after cooling to  $T_0$ ; annealed-ZFC, is the same as plain ZFC but before cooling to  $T_0$ , we apply an SCR to introduce edge contamination. The same qualitative behavior is seen in all cases: an ordered state at low temperatures undergoes a transition to a disordered state at high temperatures. We note that the onset and saturation temperatures are highest in the superheated ZFCW lattice. In the same figure, we show the data for the FC lattice that remains in a supercooled disordered state at all temperatures<sup>3</sup>.

This data demonstrate that there is an onset temperature below which excursions in temperature leave the vortex state unchanged while excursions beyond this temperature lead to an irreversible increase in  $I_{cc}(T_I)$ . We interpret these results in terms of a two-phase-coexistence model whereby the increase in  $I_{cc}(T_I)$  is caused by the introduction of disordered domains that coexist with ordered domains. This picture is consistent with recent Hall probe microscopy<sup>26</sup> and magneto-optics imaging experiments<sup>27</sup> that revealed a mixture of ordered and disordered domains in the peak region. The disordered domains

remain unchanged upon cooling, so that the cooled state is a replica of the state at  $T_1$ .

Therefore:

$$I_{cc}(T_1) = \alpha(T_1) I_{cd}(T_0) + (1 - \alpha(T_1)) I_{co}(T_0)$$

where  $\alpha(T_1)$  is the fraction of disordered phase measured along the path where vortex motion first sets in. This is a path connecting the sample edges that minimizes the amount of disordered phase and is the one that determines the value of the critical-current. Here  $I_{cd}(T_0)$  and  $I_{co}(T_0)$  are the critical currents of the disordered and ordered vortex lattice measured at  $T_0$ . From the measured  $I_{cc}(T_1)$ ,  $I_{cd}(T_0)$  and  $I_{co}(T_0)$  we obtain  $\alpha(T_1)$  and use it calculate  $I_c(T_1) = \alpha(T_1) I_{cd}(T_1) + (1 - \alpha(T_1)) I_{co}(T_1)$ , the critical current of the static vortex lattice at  $T_1$  shown in Fig. 1 by solid symbols. At high temperatures where  $I_{co}(T_1)$  is experimentally inaccessible we estimate its value by extrapolating the low temperature data (dashed line in Fig.1.). The two-phase-coexistence model gives  $\alpha(T_1) = 0$  and  $I_{cc}(T_1) = I_{co}(T_0)$ , as long as there is a contiguous sheet connecting opposite edges of the sample in which all vortices are in the ordered phase. This is true even if the sample contains islands of disordered phase. Such a sheet cannot be found when the disordered phase percolates cutting the sample lengthwise, so that  $\alpha(T_1) > 0$  and  $I_{cc}(T_1) > I_{co}(T_0)$ . Thus  $T_{on}$  marks the temperature where the disordered state percolates. Beyond this point, as  $\alpha(T_1)$  increases with temperature, so does  $I_{cc}(T_1)$ . As long as  $\alpha(T_1) < 1$  there are ordered islands embedded in the sample until they disappear at  $\alpha(T_1) = 1$  where the entire sample is disordered. For the lattice prepared by ZFCW and measured at  $T_0$ , the mechanisms of current-induced-organization are eliminated so that the disordered phase can only be nucleated by thermal fluctuations. Therefore, the limit of superheating of the ordered phase coincides with the point where the ZFCW lattice becomes completely

disordered, at  $T_s = 5.14$  K. Indeed for  $T > T_s$  we find that the vortex lattice is always disordered, regardless of the method of preparation or measurement speed, and metastability or hysteresis are absent. We conclude that it is not energetically possible for an ordered domain to exist above this temperature and therefore we identify it with the spinodal point for the superheated vortex lattice in 2H-NbSe<sub>2</sub>. By contrast we found no limit of supercooling for the FC state. By repeating the measurements for several field values we obtained the phase diagram shown in Fig. 4 in terms of the reduced variables  $t = T/T_c$  and  $h = H/H_{c2}$ . The spinodal points  $t_s$  lie on a line well separated from the critical line  $t_c$  and are significantly above the onset  $t_{on}$  and peak  $t_p$  temperatures for the FCR-ZFC lattice.

Repeating the experiments for samples B and C produced the same behavior. Both samples revealed a spinodal point for the superheated vortex lattice but no evidence for a limit of supercooling. As shown in Fig 4 the spinodal points for samples B and C lie on the same line as those of sample A even though they are from different batches, with different impurity content. This robustness suggests that the spinodal line, unlike the position of the peak or its onset, reflects a universal property of the vortex system.

We compare our results to a recent theory by Li and Rosenstein<sup>16</sup> (LR), based on a Lowest Landau Level Ginzburg-Landau approach, in which the free energies of the vortex liquid and solid are calculated and compared to high precision. In terms of the dimensionless scaled temperature,  $a_T(t, h) = - [t h (Gi)^{1/2} \pi/4]^{-2/3} [(1-t-h)/2]$ , this theory gives the melting and spinodal lines at  $a_T = -9.5$  and  $a_T = -6$  respectively. Here  $Gi = 1/8 (k_B T_c / \epsilon \epsilon_0 \xi)^2 = 9 \times 10^{-7} (T_c / 5.61)^2$  is the Ginzburg number<sup>2,15</sup>,  $\xi$  the coherence length in the a-b plane,  $\epsilon = (m_{ab}/m_c)^{1/2}$  is the anisotropy parameter and  $\epsilon_0 = (\Phi_0 / 4\pi\lambda)^2$  is the

characteristic vortex line energy . The calculated LR lines for the melting and spinodal of sample A are shown in Fig. 4. We note that the LR spinodal line practically coincides with our  $t_s(h)$  data and is well separated from both the LR melting line  $t_m(h)$  and  $t_c(h)$ . Another prediction of the LR theory is that for a system of particles with repulsive interactions as is the case of vortices, there is no limit of supercooling. This is again consistent with the data presented here.

We note that  $t_m(h)$  does not coincide with one of the characteristic peak effect features. This allows us to address a long debated question regarding the peak effect, *i.e.* whether it is the onset<sup>8,12,14,22</sup> or the peak<sup>21</sup>, which signals the phase transition. Clearly, the LR melting line coincides with neither. In the two-phase coexistence model, this is not surprising because  $T_{on}$  marks the point where the disordered phase percolates while  $T_p$  is determined by the competition between the nucleation of disordered states that tend to increase the critical current and the approach to  $T_c$ , which tends to lower it. Our experiments suggest that in transport measurements the order-disorder transition exhibits no specific signature.

The schematic free-energy diagram in Fig. 4 summarizes the results presented here. Below the spinodal line,  $t_s$ , the free energy has two minima corresponding to the disordered and ordered phases. Below the melting line  $t < t_m$  the ordered phase is stable and the disordered one metastable, while for  $t_m < t < t_s$  the roles are reversed. At  $t = t_s$  the minimum corresponding to the ordered phase is replaced by an inflection point and for  $t > t_s$  there is no minimum corresponding to an ordered domain.

Work supported by NSF-DMR and by DOE.



- <sup>1</sup> P. M. Chaikin and T. C. Lubensky, *Principles of Condensed Matter Physics*, 1st edition (Cambridge University Press, Cambridge, 1995), Vol. 1.
- <sup>2</sup> G. Blatter et al. *Rev. Mod. Phys.* **66**, 1125-1388 (1994).
- <sup>3</sup> W. Henderson, E.Y.Andrei, M. Higgins.& S. Bhattacharya, *Phys. Rev. Lett.* **77**, 2077-2080 (1996).
- <sup>4</sup> B..Saset al, *Phys. Rev. B* **61**, 9118-9121 (2000).
- <sup>5</sup> X.S. Ling, et al.,*Phys. Rev. Lett.* **86**, 712-715 (2001)
- <sup>6</sup> W. Henderson, E.Y.Andrei, M. Higgins.*Phys. Rev. Lett.* **81**, 2352-2355 (1998)
- <sup>7</sup> W.K. Kwok, et al. *Physica C* **293**, 111-117 (1997).
- <sup>8</sup> Z.L Xiao, E.Y. Andrei, P. Shuk, and M. Greenblatt, . *Phys. Rev. Lett.* **86**, 2431-2434 (2001)
- <sup>9</sup> C. J. Olson, et al *Phys. Rev. B* **67**, 184523 (2003)
- <sup>10</sup> R. Wordenweber, P. H. Kes, & C. C. Tsuei, *Phys. Rev. B* **33**, 3172-3180 (1986)
- <sup>11</sup> A. I. Larkin, and. Yu. N. Ovchinnikov, *Sov. Phys. JETP* **38**, 854-858 (1974)
- <sup>12</sup> K. W Kwok, J. Fendrich, A. C. J. van der Beek, and G. W Crabtree, *Phys. Rev. Lett.* **73**, 2614-2617 (1994)
- <sup>13</sup> C.Tang, X. S Ling, S.Bhattacharya, and P. M. Chaikin, *Europhys. Lett.* **35**, 597-602 (1996)
- <sup>14</sup> P.L. Gammel et al. *Phys. Rev. Lett.* **80**, 833-836 (1998).
- <sup>15</sup> G. P. Mikitik, and E. H. Brandt, *Phys. Rev. B* **64**, 184514 (2001)
16. D. Li, and B. Rosenstein, cond-mat/0305258; Rapid Com. PRB65, 220504 (2002), PRB65,214532(2002)
- <sup>17</sup> T. Giamarchi and P. Le Doussal, *Phys. Rev. B* **52**, 1242-1270 (1995)

- <sup>18</sup> E. Zeldov., et al. *Nature* **375**, 373-376 (1995).
- <sup>19</sup> A. Schilling, et al. *Nature*(London) **382**, 791-793 (1996)
- <sup>20</sup> S. N Gordeev,. *et al. Nature* **385**, 324-326 (1997).
- <sup>21</sup> Z. L. Xiao, E.Y. Andrei, & M. J Higgins, *Phys. Rev. Lett.* **83**, 1664-1667 (1999).
- <sup>22</sup> E. Y. Andrei, *et al. J. Phys. IV* **10**, 5-10 (1999)
- <sup>23</sup> Paltiel. Y.*et al.*, *Nature* **403**, 398-401 (2000)
- <sup>24</sup> Z. L.Xiao, , E. Y Andrei, Y.Paltiel, E. Zeldov, P.Shuk, , and M. Greenblatt,  
*Phys. Rev. B* **65**, 094511 (2002)
- <sup>25</sup> A. V Koshelev., and V. L. Vinokur, *Phys. Rev. Lett.* **73**, 3580-3583 (1994)
- <sup>26</sup> M.Marchevsky, M. J. Higgins, and S. Bhattacharya, *Nature* **409**, 591-594 (2001)
- <sup>27</sup> Soibel, A. *et al. Nature* **406**, 282-287 (2000)

**Figure 1. The Peak Effect. Temperature dependence of critical currents at  $H=0.3\text{ Tesla}$ : open squares: usual peak effect obtained with a slow current ramp for the zero field cooled (ZFC) lattice; open triangles: fast measurement of ZFC state; open circles: fast measurement for the zero field cooled and warmed (ZFCW) lattice; solid circles: calculated values from data in Fig.3 for the ZFCW lattice. The arrows indicate the direction of decay of the metastable supercooled FC state and the superheated ZFCW state. Inset: field-temperature trajectories used in lattice preparation and measurement.**

**Figure 2. Current-driven-organization. Voltage-current (V-I) curves for the ZFCW lattice at  $H=0.3\text{T}$  in sample A close to the peak temperature  $T_p=5.0\text{ K}$ . The N-shaped curves are a signature of current induced organization.**

**Figure 3. Suprheating and supercooling measured in the absence of current induced organization. The cold-measured critical currents  $I_{cc}$ , are shown for different vortex lattices prepared at the target temperature  $T_1$  and measured at  $T_0=4.4\text{K}$  as described in the text. The FC data represents a supercooled disordered state and the ZFCW data a superheated ordered state.  $T_s$  is the limit of metastability for the ordered state.  $T_{on}$  is the temperature were the disordered domains percolate across the sample in the ZFC lattice.**

**Figure 4. Phase diagram for the vortex lattice in  $2\text{H-NbSe}_2$ . The measured spinodal points (circles) are compared with the spinodal line calculated from the Li**

**&Rosenstein theory<sup>15</sup> (dashed-dot line) for sample A (  $T_c=5.6\text{K}$ ,  $H_{c2}=4.7\text{ Tesla}$ ).**  
**The calculated lines for samples B ( $T_c=7.0\text{K}$ ,  $H_{c2}=5.4\text{ Tesla}$ ) and C ( $T_c=6.0\text{K}$ ,  $H_{c2}=5.3\text{Tesla}$ ) are included within the line thickness. The calculated melting line<sup>16</sup> (dashed line) lies well above the measured peak (triangles) and onset (diamonds) temperatures. The schematic free energy diagrams show the relative depth of the minima of the disordered (D) and ordered (O) phases in each regime.**

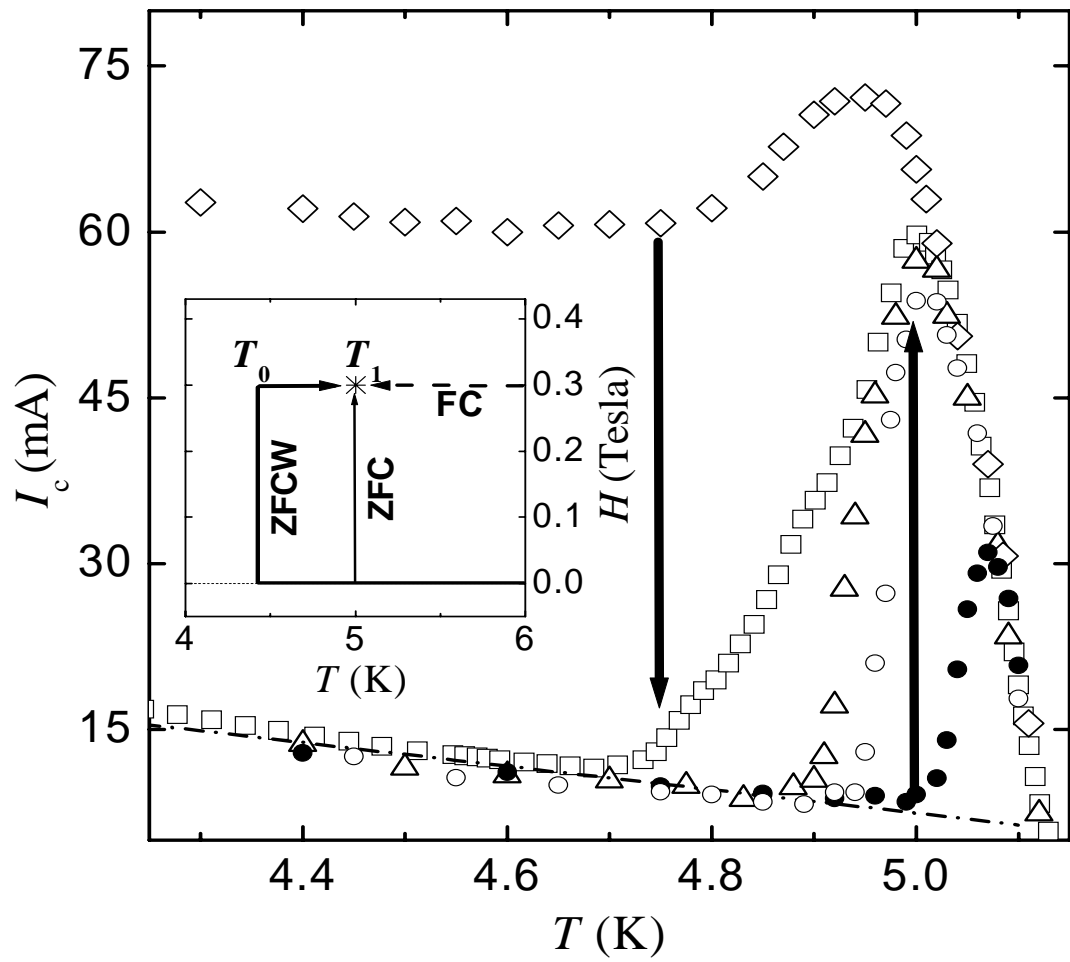


Figure 1.

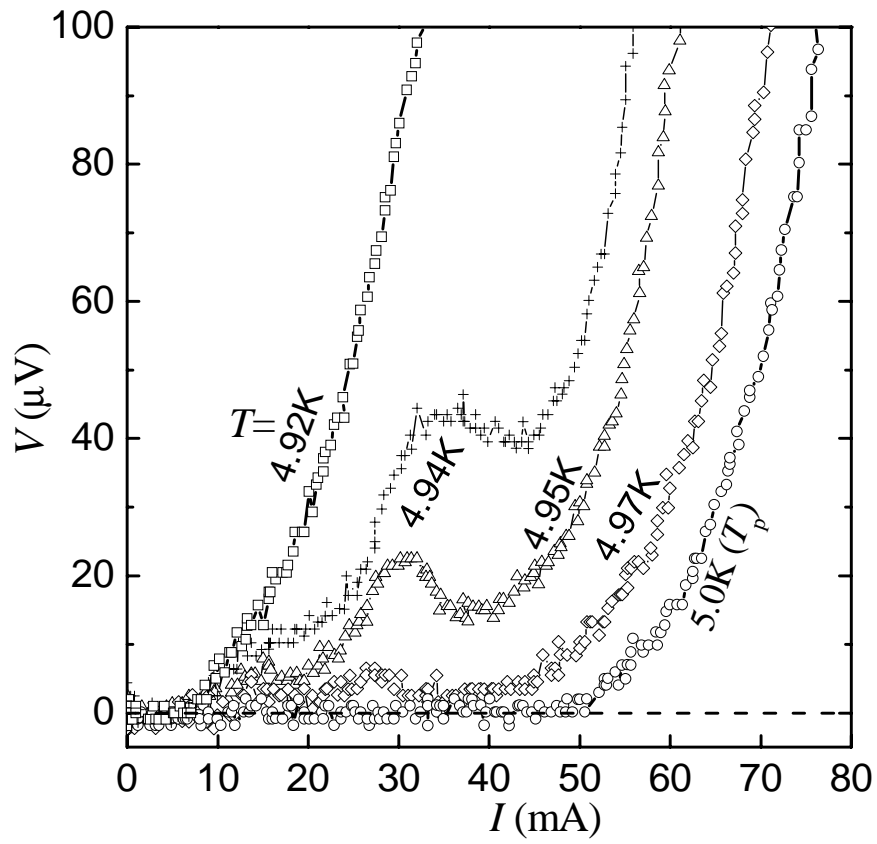


Figure 2.

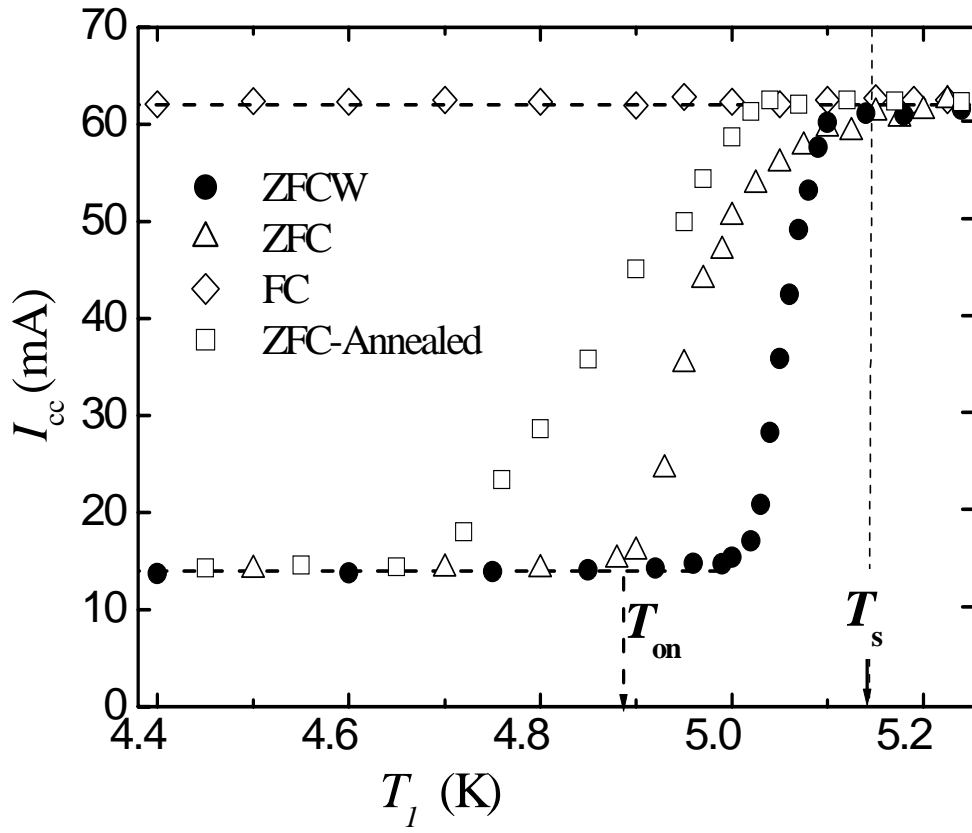


Figure 3.

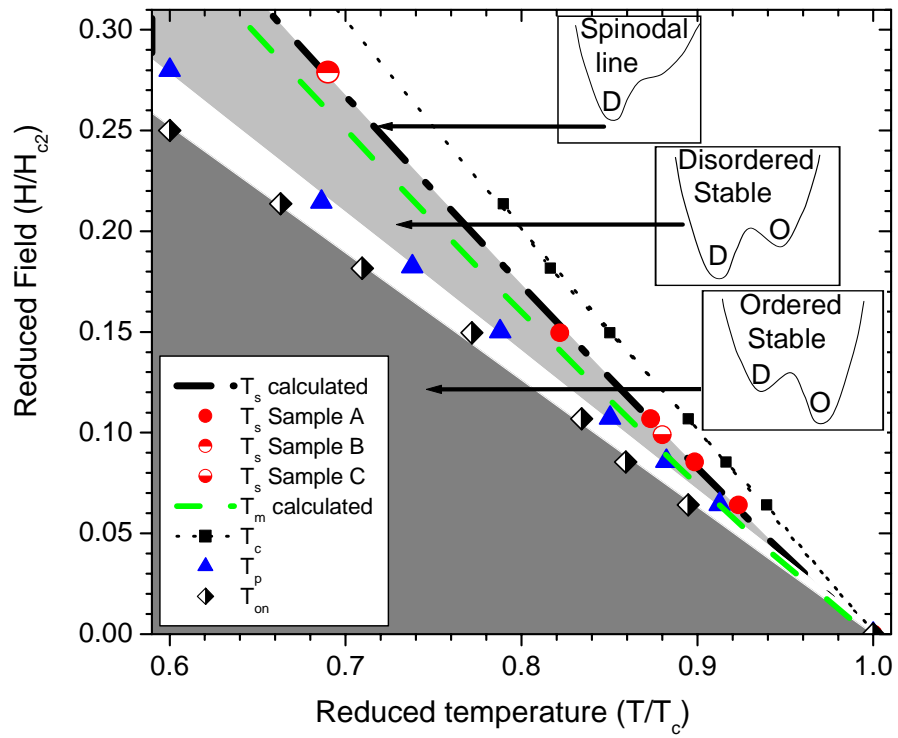


Figure 4.